The American Journal of Pathology, Vol. 184, No. 9, September 2014

The American Journal of
PATHOLOGY
ajp.amjpathol.org

IMMUNOPATHOLOGY AND INFECTIOUS DISEASES

Complement Regulatory Protein CD46 Protects against Choroidal Neovascularization in Mice

Valeriy Lyzogubov,* Xiaobo Wu,† Purushottam Jha,* Ruslana Tytarenko,* Michael Triebwasser,† Grant Kolar,†‡ Paula Bertram,† Puran S. Bora,* John P. Atkinson,† and Nalini S. Bora*

From the Department of Ophthalmology, Pat and Willard Walker Eye Research Center, Jones Eye Institute, University of Arkansas for Medical Sciences, Little Rock, Arkansas; the Division of Rheumatology,† Department of Medicine, and the Department of Pathology and Immunology,‡ Washington University School of Medicine, St. Louis, Missouri*

Accepted for publication
June 4, 2014.

Address correspondence to Nalini S. Bora, Ph.D., Department of Ophthalmology, Jones Eye Institute, University of Arkansas for Medical Sciences, 4301 W. Markham, #523-7, Little Rock, AR 72205-7199. E-mail: nbora@uams.edu.

Dysregulation of the complement system is increasingly recognized as a contributing factor in age-related macular degeneration. Although the complement regulator CD46 is expressed ubiquitously in humans, in mouse it was previously thought to be expressed only on spermatozoa. We detected CD46 mRNA and protein in the posterior ocular segment (neuronal retina, retinal pigment epithelium, and choroid) of wild-type (WT) C57BL/6J mice. *Cd46*$^{-/-}$ knockout mice exhibited increased levels of the membrane attack complex and of vascular endothelial growth factor (VEGF) in the retina and choroid. The *Cd46*$^{-/-}$ mice were also more susceptible to laser-induced choroidal neovascularization (CNV). In *Cd46*$^{-/-}$ mice, 19% of laser spots were positive for CNV at day 2 after treatment, but no positive spots were detected in WT mice. At day 3, 42% of laser spots were positive in *Cd46*$^{-/-}$ mice, but only 11% in WT mice. A fully developed CNV complex was noted in both *Cd46*$^{-/-}$ and WT mice at day 7; however, lesion size was significantly ($P < 0.05$) increased in *Cd46*$^{-/-}$ mice. Our findings provide evidence for expression of CD46 in the mouse eye and a role for CD46 in protection against laser-induced CNV. We propose that the *Cd46*$^{-/-}$ mouse has a greater susceptibility to experimental CNV because of insufficient complement inhibition, which leads to increased membrane attack complex deposition and VEGF expression. *(Am J Pathol 2014, 184: 2537–2548; http://dx.doi.org/10.1016/j.ajpath.2014.06.001)*

Age-related macular degeneration (AMD) is a leading worldwide cause of central vision loss in individuals over the age of 50.[1–5] The prevalence of AMD is growing because of increased longevity. The disease brings negative changes in life style. AMD patients often cannot perform daily tasks of living, such as reading or driving. Current estimates are that it requires 575 to 733 million dollars annually to treat AMD in the United States.[5] Thus, AMD profoundly affects the quality of life, creating a serious social and public health problem.[3,4]

Two major clinical phenotypes of AMD are recognized: nonexudative (dry type) and exudative (wet type). Wet AMD is frequently associated with central blindness, and choroidal neovascularization (CNV) is the hallmark of this type in humans. Agents available for treating exudative AMD reduce the rate of vision loss, but they do not reverse damage; furthermore, they are associated with a variety of ocular complications, require repetitive administration, and are expensive.[1–4]

AMD is a disease with numerous risk factors, and multiple pathological mechanisms have been reported.[6–10] Evidence accumulated during the past decade, primarily through genetic studies, strongly indicates that the alternative pathway of the complement system plays an important role in AMD pathogenesis in humans.[3,11–15] Reports from multiple investigators have established that the membrane attack complex (MAC) C5b-9, formed as a result of

Supported by grants from the Edward N. & Della L. Thome Memorial Foundation, the Lions of Arkansas Foundation, and the Pat and Willard Walker Eye Research Center–Harvey & Bernice Jones Eye Institute and by NIH grants R01-AI041592 (J.P.A.), R01-GM099111 (J.P.A.), P20-RR016460 (Digital Microscopy Core), P30-DK052574 (Morphology Core), and P30-AR048335 (Protein Production and Purification Core Facility–Rheumatic Diseases Core Center).

The content is solely the responsibility of the authors and does not necessarily represent the official views of the NIH.

Disclosures: None delcared.

http://dx.doi.org/10.1016/j.ajpath.2014.06.001

alternative pathway complement engagement, participates in mediating animal models of CNV.[11,12,16–23] Complement regulatory proteins control the complement cascades,[24,25] and their deficiency has been reported to predispose to the development of experimental CNV.[18,20]

CD46 [alias membrane cofactor protein (MCP)] is a widely expressed transmembrane glycoprotein in primates that serves as a complement regulatory protein[26,27] and is present in the normal human eye.[28–31] It binds C3b and C4b and then serves as a cofactor protein for the cleavage of these two substrates by serine protease factor I. In rodents, however, CD46 expression has been firmly established only for the inner acrosomal membrane of spermatozoa.[32–34] Our goal in the present study was to investigate whether CD46 is expressed in the mouse eye. After this was unequivocally shown, we explored its role in a murine model of laser-induced CNV.[11,12,35,36]

Materials and Methods

Animals

A mouse with homozygous deficiency of *Cd46* (*Cd46*$^{-/-}$) on the C57BL/6J background was generated at the Washington University School of Medicine in St. Louis. Standard targeting techniques[37] were used to replace complement control protein repeat 1 (CCP 1) and almost all of the CCP 2a sequence of the mouse *Cd46* gene with the Neo cassette. Southern blotting with a probe between CCP 2b and CCP 3 was used to confirm targeted embryonic stem cells (129Sv origin; Washington University Cancer Center). Positive embryonic stem-cell clones were expanded and microinjected into blastocyst-stage embryos of C57BL/6J mice. The embryos were next transferred into the uterus of surrogate females. Germline transmission of the disrupted *Cd46* gene was noted in chimeric mice, and the resultant heterozygotes were bred to produce three genotypes: homozygous, heterozygous, and wild-type (WT) mice. The phenotype was unaltered, and reproductive capacity was normal.

Homozygous knockout mice were subsequently backcrossed into C57BL/6J for at least eight generations. Neo primers were used to detect the targeted band, and CD46 primers (CD46 primer A: 5′-ATGCCTGTGAACTACCACGGCCATTTGAAG-3′; CD46 primer B: 5′-AACTTTAATATAGCTCCAGTGCCAGTTGCA-3′) were used to detect the deleted sequences. Genotypes of mice were determined by PCR analysis of tail-derived DNA. Male homozygous *Cd46*$^{-/-}$ mice, 6 to 8 weeks of age, were used. Age- and sex-matched C57BL/6J mice purchased from the Jackson Laboratory (Bar Harbor, ME) served as a WT control.

Preparation of Polyclonal Anti-CD46 Antibody

Using cDNA prepared from C57BL/6J mouse testes as a template, full-length murine CD46 was amplified using the following oligos: 5′-CGCGGATCCATGACGGCGGCGCCTCTTAT-3′ and 5′-ATAAGAATGCGGCCGCTCATCTTGCTGCAGATACATTTG-3′. The resulting PCR fragment was ligated into the BamHI and NotI sites of pET28a(+)-2, a derivative generated in our laboratory of pET-28a(+) (Novagen; EMD Millipore, Billerica, MA). This plasmid was then used as a template to generate murine CD46 CCPs 1 and 2 and murine CD46 CCPs 3 and 4 separately, using the following oligos: 5′-CGCGGATCCATGGATGCCTGTGAACTACC-3′ and 5′-ATAAGAATGCGGCCGCTTATTCACAATGTGGGGGATAGC-3′ for CCPs 1 and 2, and 5′-CGCGGATCCATGAAGATTTATTGTTTACCACCTC-3′ and 5′-ATAAGAATGCGGCCGCTTATTTAAGACATTTTGGGATAGAT-3′ for CCPs 3 and 4. The resulting PCR fragments were ligated into the BamHI and NotI sites of pET28a(+)-2. The recombinant proteins were expressed and purified as described previously.[38] Refolded CCP 1 and 2 and CCP 3 and 4 proteins were pooled and then purified over a Superose 12 sizing column (GE Healthcare, Little Chalfont, UK). Pooled proteins were injected into rabbits for polyclonal antibody (Ab) generation (Harlan Laboratories, Indianapolis, IN).

RT-PCR Analysis

Total RNA was extracted from the posterior segment of eyes [ie, neuronal retina, retinal pigment epithelium (RPE), and choroid] and testes of WT and *Cd46*$^{-/-}$ mice for RT-PCR using an RNeasy kit (Qiagen, Valencia, CA). Specific oligonucleotide primers derived from the mouse *Cd46* gene (National Center for Biotechnology Information; *http://www.ncbi.nlm.nih.gov/nuccore/NM_010778*; accession number NM_010778) were synthesized at Integrated DNA Technologies (Coralville, IA). RT-PCR was performed using the following primers: mouse β-actin, 5′-GGCTGTATTCCCCTCCATCG-3′ (forward) and 5′-AGCCTGGATGGCTACGTACA-3′ (reverse); mouse CD46, 5′-ATGCCTGTGAACTACCACGGCCATTTGAAG-3′ (forward) and 5′-TTTGCCAAATGAAGGGTCTTG-3′ (reverse). RT-PCR for CD46 and β-actin transcripts was performed using 0.1 μg of total RNA as template, with reagents purchased from Bio-Rad Laboratories (Hercules, CA). PCR was performed using 27, 29, and 35 cycles. The negative control reactions included nuclease-free water (Ambion; Life Technologies, Carlsbad, CA) instead of the RNA and a reaction lacking reverse transcriptase.

Western Blot Analysis

Tissues harvested from the neuronal retina, RPE, and choroid of WT and *Cd46*$^{-/-}$ mice were homogenized and solubilized in ice-cold phosphate-buffered saline containing 1% protease inhibitors and 1% NP-40 (Sigma-Aldrich, St. Louis, MO). Electrophoresis was performed on 12% SDS–polyacrylamide gels with 20 μg of total protein loaded in each lane. The separated proteins were transferred to polyvinylidene difluoride membranes. The blots were blocked with 5% bovine serum albumin overnight at 4°C. A rabbit polyclonal IgG reactive with mouse C9

(dilution 1:40,000) provided by Prof. Brian P. Morgan (University of Wales College of Medicine, Cardiff, UK) and a monoclonal IgG to β-actin (dilution 1:10,000; Sigma-Aldrich) were used as the primary Abs. The blots were treated separately with these Abs at room temperature for 2 hours. The anti-C9 Ab recognizes neoepitopes on C9 in the MAC.[16–18] Horseradish peroxidase–labeled goat anti-rabbit IgG and horseradish peroxidase–labeled goat anti-mouse IgG (both from Santa Cruz Biotechnology, Dallas, TX) were used as the secondary Abs for C9 and β-actin, respectively. Blots were developed using an enhanced chemiluminescence Western blotting detection system (Pierce SuperSignal West Femto; Thermo Fisher Scientific, Waltham, MA), according to the manufacturer's recommendations. Quantification of protein bands was accomplished by analyzing the intensity of the bands using ImageJ software version 1.46r (NIH, Bethesda, MD).

ELISA

For enzyme-linked immunosorbent assay (ELISA), neuronal retina, RPE, and choroid tissues were harvested from enucleated eyes of WT and *Cd46*$^{-/-}$ mice. The tissue sample was placed in 500 μL of lysis buffer and homogenized on ice for 30 seconds; the lysate was then centrifuged at 9 × *g* for 10 minutes at 4°C. Levels of VEGF protein in the supernatant were determined using a mouse VEGF ELISA kit (R&D Systems, Minneapolis, MN). The assay was performed according to the manufacturer's recommendations. Samples were analyzed in duplicate.

Immunohistochemical Studies

Immunoperoxidase Staining

Mouse epididymis was cut in 8-μm sections using a CM 1850 cryostat (Leica Microsystems, Wetzlar, Germany). Sections were fixed with 95% ethanol and 5% glacial acetic acid for 10 minutes at room temperature. The endogenous peroxidases were blocked by H_2O_2 (1.5%) in methanol for 30 minutes at room temperature. Sections were treated with avidin and biotin blocking solutions (Vector Laboratories, Burlingame, CA) for 15 minutes each. Tissues were incubated with blocking solution (10% goat serum, 10% mouse serum, and 1% bovine serum albumin in phosphate-buffered saline) for 60 minutes at room temperature. Rabbit anti-mouse CD46 at 4.2 μg/mL in blocking solution was added to stain the sections for 60 minutes at room temperature. After three washes with phosphate-buffered saline, sections were incubated with 1:200 dilution of biotinylated goat anti-rabbit IgG (Jackson ImmunoResearch Laboratories, West Grove, PA) for 60 minutes at room temperature. Sections were subsequently incubated with an avidin–biotin peroxidase complex (ABC complex; Vector Laboratories) for 60 minutes at room temperature. Tissue structures were visualized with ImmPACT 3,3′-diaminobenzidine substrate (Vector Laboratories).

Immunofluorescence Staining

Identification and Localization of CD46 in Mouse Eye

Eyes and testes harvested from WT and *Cd46*$^{-/-}$ mice were placed in Tissue-Tek OCT optimal cutting temperature compound (Sakura Finetek, Torrance, CA), snap-frozen, and stored in sealed vials at −80°C until sectioning by cryostat. Tissue sections (8 μm thick) were fixed in 95% ethanol and 5% glacial acetic acid (Thermo Fisher Scientific) for 20 minutes at −20°C. Sections were incubated in 1% bovine serum albumin (Thermo Fisher Scientific) and 10% donkey serum (Jackson ImmunoResearch Laboratories) for 30 minutes to block nonspecific binding. Tissue sections were treated with rabbit polyclonal anti-mouse CD46 Ab (dilution 1:400) for 18 hours at 4°C. DyLight 549–conjugated anti-rabbit IgG (donkey) (dilution 1:400; Jackson ImmunoResearch Laboratories) served as the secondary Ab.

To identify Müller cells in the retina and cells of mesenchymal origin in the testis, the sections were treated with rabbit anti-vimentin monoclonal Ab conjugated with Alexa Fluor 488 (dilution 1:200; Cell Signaling Technology, Danvers, MA). Mouse monoclonal anti–cytokeratin 18 (anti–CK-18) primary Ab (ABR; Thermo Fisher Scientific), goat anti-mouse Alexa Fluor 488–conjugated secondary Ab (Life Technologies), and a M.O.M. (mouse-on-mouse) immunodetection kit (Life Technologies) were used to identify RPE cells. Control stains were performed with an isotype-matched Ab at a concentration equal to that of the primary Ab. Additional controls included omitting the primary or secondary Ab. Anti-CD46 polyclonal Ab, blocked with excess recombinant CD46 protein (purified mouse CD46 CCPs 1 and 2 and mouse CD46 CCPs 3 and 4) was also used as control. Sections were mounted in ProLong antifade reagent with DAPI (Life Technologies) and examined using an LSM510 laser confocal microscope (Carl Zeiss Microscopy, Jena, Germany). Beam splitters were set up as follows: 405 nm laser (10%) window 420 to 480 nm, 488 nm laser (10%) window 505 to 530 nm, and 561 nm laser (15%) window 575 to 615 nm. Eight-bit images were obtained using the microscope in sequential mode with line average of 8 and a format of 1024 × 1024 pixels. We captured a single 1-μm optical slice of each section using an EC Plan-Neofluar 40×/1.30 oil differential interference contrast (DIC) objective or a Plan-Apochromat 63×/1.4 oil DIC objective. All images were captured with the same settings. DIC images were captured to facilitate localization of histological structures of the eye. Cryosections from the eyes were also stained with hematoxylin and eosin and investigated using a Vanox-S microscope (Olympus, Tokyo, Japan) equipped with a GO-5 camera (QImaging, Surrey, BC, Canada). Images of hematoxylin and eosin–stained sections were captured using an SPlan 40×/0.7 objective (Olympus).

MAC Deposition and VEGF Expression

Eyes harvested from WT and *Cd46*$^{-/-}$ mice were fixed in 10% neutral buffered formalin (Sigma-Aldrich) for 4 hours at 25°C. Eyes were embedded in paraffin, and 5-μm sections were cut. After deparaffinization in xylene and rehydration, sections

were treated with antigen unmasking solution (Vector Laboratories). All samples were processed at the same time. For detection of the MAC, sections were treated with rabbit polyclonal anti-MAC (C9 neoepitope) Ab (primary Ab), followed by Alexa Fluor 594–conjugated donkey anti-rabbit IgG [(heavy chain and light chain) (secondary Ab) (Life Technologies). For VEGF staining, we used rabbit polyclonal anti-VEGF (Abcam, Cambridge, MA) as the primary Ab and Alexa Fluor 594–conjugated goat anti-rabbit (Life Technologies) as the secondary Ab. Müller cells in the retina were identified as described above. Mouse monoclonal anti–CK-18 (primary Ab) (ABR; Thermo Fisher Scientific), goat anti-mouse Alexa Fluor 488–conjugated (secondary Ab) (Life Technologies), and a M.O.M. immunodetection kit (Life Technologies) was used to identify RPE cells. Sections were examined with an LSM510 laser confocal microscope (Zeiss) using settings as described above.

Induction and Measurement of CNV and VEGF Expression in Laser Spots

CNV was induced by laser photocoagulation with an argon laser (spot size, 50 μm; duration, 0.05 seconds; power, 260 mW) as described previously.[16–23] Three laser spots were placed in each eye, close to the optic disk. Production of a vaporization bubble at the time of laser confirmed the rupture of Bruch's membrane. Mice were anesthetized with a ketamine/xylazine cocktail at days 2, 3, and 7 after laser treatment. They were then perfused with 0.75 mL of phosphate-buffered saline containing 50 mg/mL of fluorescein isothiocyanate–labeled dextran (2×10^6 molecular weight) (Sigma-Aldrich) before sacrifice. The eyes were harvested and fixed for 4 hours in 10% neutral buffered formalin (Sigma-Aldrich), and RPE–choroid–scleral flat mounts were prepared.[16–23] For VEGF staining, we used rabbit polyclonal anti-VEGF (Abcam, Cambridge, MA) as the primary Ab and Alexa Fluor 594–conjugated goat anti-rabbit (Life Technologies) as the secondary Ab. The flat mounts were mounted in ProLong antifade reagent (Life Technologies) with the sclera facing down and were examined under an LSM510 confocal microscope (Zeiss). In confocal micrographs, areas of green fluorescence (CNV complex size) or red fluorescence ($VEGF^+$ staining) in laser spots were measured using NIH ImageJ software. Laser spots were identified by staining for filamentous actin using Alexa Fluor 647–conjugated phalloidin (Life Technologies). If the CNV was $\leq$3% of the total laser spot area, it was graded negative; CNV of >3% was graded positive.

Ethics

The knockout mouse was generated under an animal protocol approved by the Division of Comparative Medicine at Washington University in St. Louis. Animal experiments were approved by the Institutional Animal Care and Use Committee, University of Arkansas for Medical Sciences, Little Rock.

Statistical Analysis

Data were analyzed and compared using the *U*-test or analysis of variance, and differences were considered statistically significant at $P < 0.05$.

Results

Generation of the *Cd46*$^{-/-}$ Mouse

To generate a CD46 knockout mouse, the *Cd46* gene was disrupted, as described under *Materials and Methods*. A positive ES clone is shown in Figure 1A. PCR reactions of mouse tail DNA were performed to distinguish the three genotypes (Figure 1B). Analysis with a polyclonal anti-mouse CD46 Ab was used to verify the absence of CD46 protein in the epididymis of the *Cd46*$^{-/-}$ mice (Figure 1C). These results demonstrated that inactivation of the mouse *Cd46* gene was complete. Homozygous *Cd46*$^{-/-}$ mice were viable, developed normally, and were fertile.

Expression of CD46 mRNA and Protein in the Posterior Segment of the Mouse Eye

RT-PCR was used to detect CD46 mRNA in the retina and choroid of eyes from WT and *Cd46*$^{-/-}$ mice. Testes were

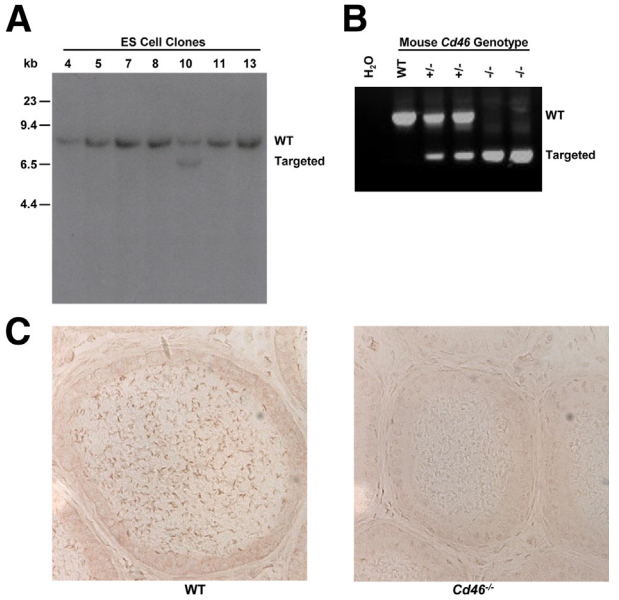

Figure 1 Generation of the *Cd46*$^{-/-}$ mouse. **A:** Targeted homologous recombination, as identified by Southern blot analysis of PvuII-digested DNA samples extracted from ES cell clones. Two DNA fragments, WT 9.3 kb and targeted 6.6 kb, are identified by a probe with sequences from CCP 2b to CCP 3 of the *Cd46* gene. Positive ES clones (such as number 10) were injected into C57BL/6J blastocysts to generate chimeric mice. **B:** Genotype analysis of mouse tail DNA with Neo and CD46 primers. A combination of these primers is capable of distinguishing WT, heterozygous, and homozygous mice. **C:** Immunohistochemical staining of the epididymis from WT and *Cd46*$^{-/-}$ mice with rabbit anti-mouse CD46 Ab. CD46 protein was detected in WT spermatozoa, but not in spermatozoa of the *Cd46*$^{-/-}$ mice. CCP, complement control protein (repeat or module); WT, wild type.

harvested from WT mice to serve as a positive control. Using RT-PCR, we detected CD46 mRNA in the eye and testis of WT mice, which was absent in the eye and testis of *Cd46*$^{-/-}$ mice (Figure 2A). These findings establish a second tissue site for the expression of CD46 in mouse.

The specific location of CD46 in the eye was assessed by immunofluorescence (IF) using rabbit polyclonal anti-mouse CD46 Ab. In WT mice, an intense signal for CD46 was observed on the basolateral surface of RPE cells (Figure 2, B–D) and, as expected, in the testis (Figure 2I). RPE cells were identified by staining for the intermediate filament protein CK-18 (Figure 2, B and D). Less intense staining was present in the choroid of WT mice (Figure 2, B and C). No positive signal was detected in the same structures of WT mice stained using primary Ab blocked with recombinant protein (Figure 2E), with the primary Ab omitted, (Figure 2F), or stained with rabbit nonimmune serum (Figure 2, G and J), and likewise no positive signal was detected in *Cd46*$^{-/-}$ mice (Figure 2, H and K).

Differential expression of CD46 was also observed in the WT retina (Figure 3). Hematoxylin and eosin–stained sections were used to demonstrate the choroid and layers of the retina (Figure 3E). Moderate CD46 expression was observed in the inner plexiform layer, outer plexiform layer, inner

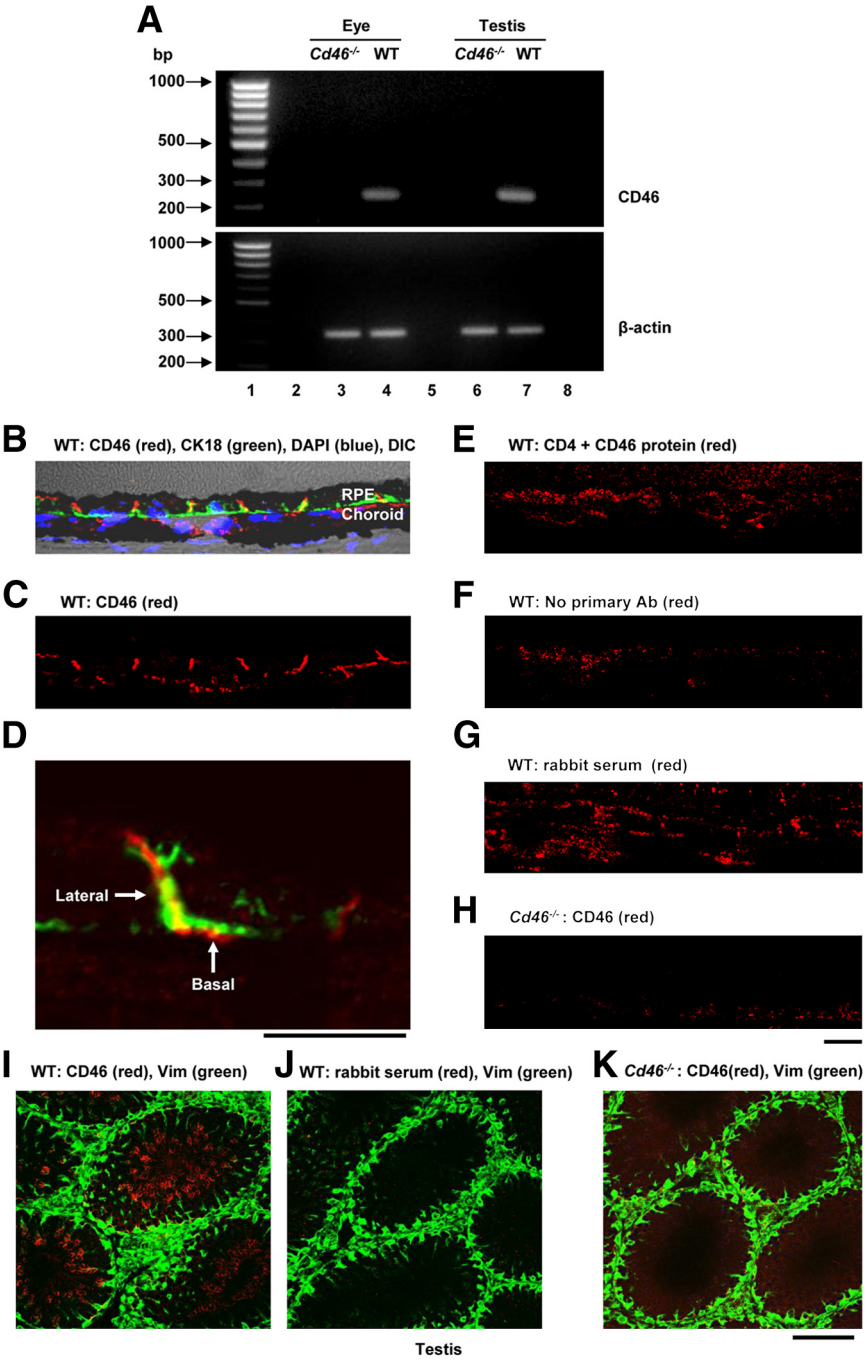

Figure 2 CD46 expression and localization in the mouse eye. **A:** CD46 mRNA was analyzed in the retina and the choroid of C57BL/6J (WT) and *Cd46*$^{-/-}$ mice. Representative ethidium bromide–stained gel shows CD46 (230 bp) transcripts in the retina and choroid (lane 4) and testis (lane 7) of WT mice. CD46 mRNA was not detected in the eye (lane 3) or testis (lane 6) of *Cd46*$^{-/-}$ mice. β-Actin (330 bp) was used as a loading control in the eye (lanes 3 and 4) and testis (lanes 6 and 7) of WT and *Cd46*$^{-/-}$ mice. Size markers (100 bp DNA ladder, lane 1). Lane 2, nuclease free water; lane 5, without reverse transcriptase, and lane 8, empty. **B–K:** For IF analysis, frozen sections were stained with rabbit polyclonal anti-CD46 Ab, CK-18, or vimentin. DIC microscopy was used to identify ocular structures on sections from WT mice. Nuclei were counterstained with DAPI. Confocal micrographs show staining for CD46 on the basolateral surface of RPE cells (**B**, **C**, and **D**), in choroid (**B** and **C**), and in testis (**I**) of WT mice. No staining was observed in the negative controls stained using a primary Ab blocked with recombinant protein (**E**), by omitting the primary Ab (**F**), or with rabbit nonimmune serum (**G** and **J**), nor in *Cd46*$^{-/-}$ mice (**H** and **K**). Results shown are representative of five independent experiments. Scale bars: 80 μm (**I–K**); 25 μm (**B**, **C**, and **E–H**); 10 μm (**D**). RPE, retinal pigment epithelium; Vim, vimentin; WT, wild type.

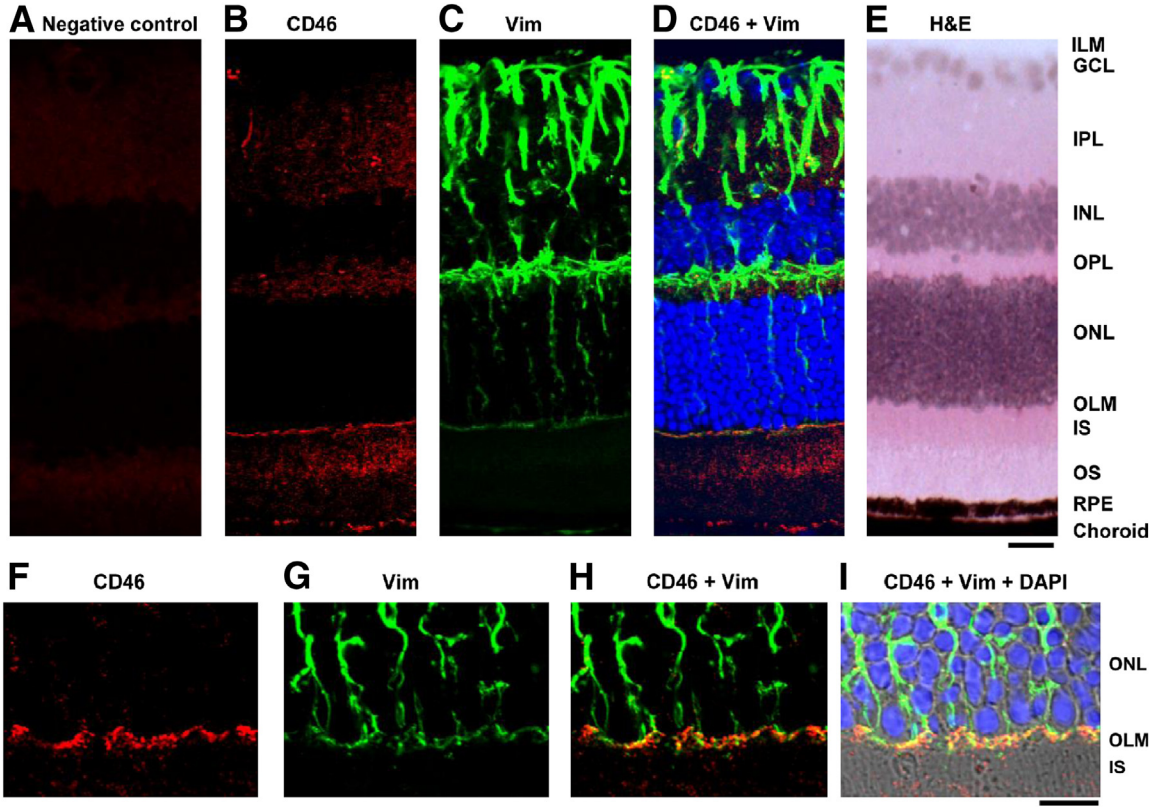

Figure 3 CD46 expression in the mouse retina. **A:** *Cd46*$^{-/-}$ mouse retina served as a negative control. **E:** Retinal layers and choroid (hematoxylin and eosin). **B**, **C**, **F**, and **G:** Frozen sections of eyes from WT C57BL/6J mice were subjected to IF staining with rabbit polyclonal Abs to CD46 (**B** and **F**) and vimentin (**C** and **G**). CD46^{+} signal (red) was detected in the neuronal retina and RPE (**B** and **F**). **D** and **H:** CD46 colocalized with vimentin. Within the neuronal retina, the most intense staining was detected in the processes of vimentin^{+} (green) Müller cells in the OLM (**D** and **H**). **I:** Confocal micrographs were merged with DIC images. Nuclei were counterstained with DAPI (blue). Images are representative of five independent experiments. Scale bars: 20 μm (**A**–**E**); 10 μm (**F**–**I**). GCL, ganglion cell layer; ILM, inner limiting membrane; INL, inner nuclear layer; IPL, inner plexiform layer; IS, inner segment of photoreceptors; OLM, outer limiting membrane; ONL, outer nuclear layer; OPL, outer plexiform layer; OS, outer segment of photoreceptors; RPE, retinal pigment epithelium; Vim, vimentin.

segment of photoreceptors, and outer segment of photoreceptors (Figure 3, B and F). Intense staining for CD46 was noted in the outer limiting membrane (OLM) (Figure 3, B and F). By contrast, the inner limiting membrane(ILM), ganglion cell layer, inner nuclear layer, and outer nuclear layer were negative for CD46 (Figure 3, B and F). Weak background staining was observed in the retinal sections of *Cd46*$^{-/-}$ mice (Figure 3A). Using IF analysis, we identified the intermediate filament protein vimentin in radial processes of Müller cells (Figure 3, C and G). CD46 colocalized with vimentin^{+} Müller cells (Figure 3D), especially in the OLM (Figure 3H). Thus, CD46 is expressed in multiple specific locations in the mouse eye.

Role of CD46 in Laser-Induced CNV

In view of these results and previous findings of an important role for complement activation in the development of laser-induced CNV,[16–18,20,21,23] we studied the response of the *Cd46*$^{-/-}$ mouse to laser injury. CNV was induced by photocoagulation using an argon laser, and mice were sacrificed at days 2, 3, and 7 after laser treatment. Confocal analyses of RPE–choroid–scleral flat mounts revealed that *Cd46*$^{-/-}$ mice were more susceptible to laser-induced CNV than WT mice. For example, at day 2 after laser treatment, 19% of the laser spots were positive for CNV, compared with 0% in WT mice (Figure 4A). At day 3 after laser treatment, 42% of the laser spots had developed CNV in *Cd46*$^{-/-}$ mice, compared with 11% in WT mice (Figure 4A), but CNV size did not differ significantly between groups (Figure 4, B–D). All spots were positive for CNV at day 7 (Figure 4A), but *Cd46*$^{-/-}$ mice had developed significantly more severe CNV ($P < 0.05$) (Figure 4, E–G).

We compared VEGF expression in laser spots at days 3 and 7 after laser treatment in *Cd46*$^{-/-}$ and WT mice, using IF analysis. We noted significantly increased VEGF^{+} staining in laser spots at day 3 (Figure 5, A–C) and at day 7 (Figure 5, D–F) after laser treatment in *Cd46*$^{-/-}$ mice, compared with WT mice ($P < 0.05$).

Underlying Mechanism Responsible for Increased Susceptibility of the *Cd46*$^{-/-}$ Mouse to CNV

This mouse model of CNV is dependent on complement activation. MAC deposition leads to the release of angiogenic growth factors, including VEGF, that drive neovascularization.

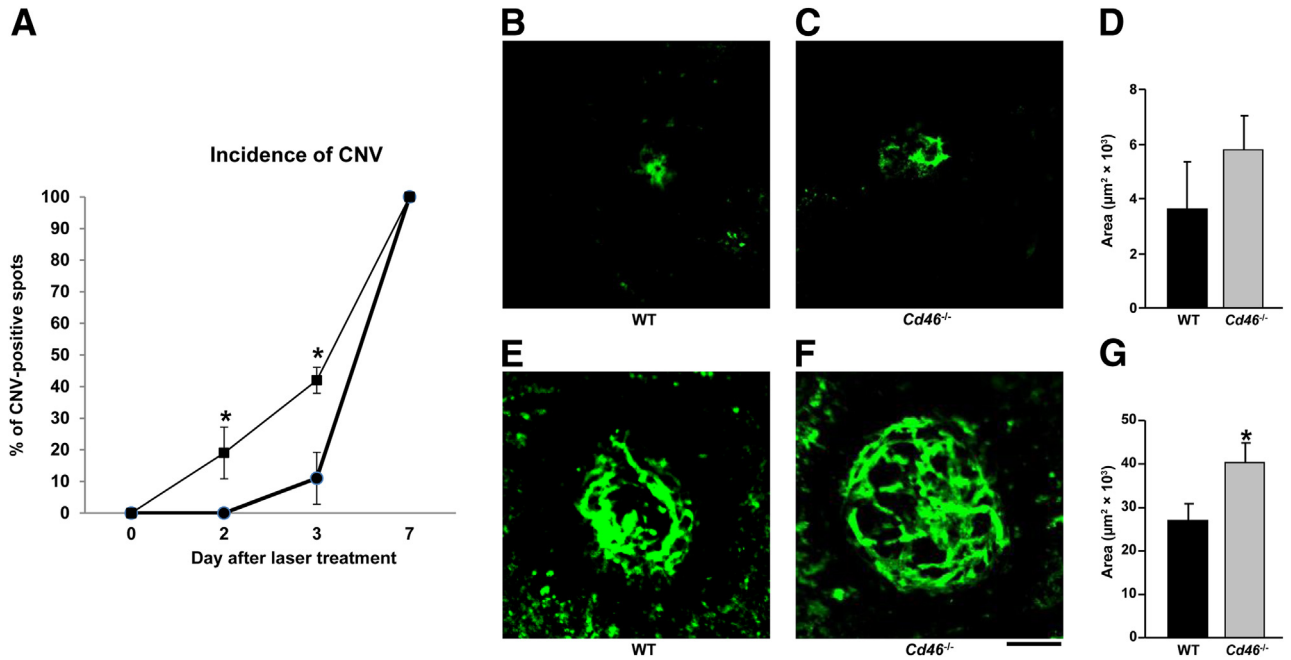

Figure 4 Effect of CD46 on the incidence of CNV and the size of CNV complex. **A:** CNV was induced in both eyes of C57BL/6J (WT; circles) and *Cd46*$^{-/-}$ (squares) mice by laser photocoagulation. Increased incidence of CNV was observed at days 2 and 3 after laser treatment in *Cd46*$^{-/-}$ mice, compared with WT mice. **B**–**G:** Representative confocal photomicrographs of RPE–choroid–scleral flat mounts with fluorescein isothiocyanate–dextran perfused vessels (green) from WT (**B** and **E**) and *Cd46*$^{-/-}$ (**C** and **F**) mice, with cumulative data of CNV quantification (**D** and **G**). At day 3 after laser treatment, the size of the CNV complex in *Cd46*$^{-/-}$ mice (**C** and **D**) is not significantly different from those in WT (**B** and **D**). However, at day 7 after laser treatment, the CNV complex is significantly larger in *Cd46*$^{-/-}$ mice (**F** and **G**), compared with WT mice (**E** and **G**). Data are expressed as means ± SEM, representative of two independent experiments. $n = 3$ mice per group at each post-treatment time point. *$P < 0.05$, analysis of variance. Scale bar = 100 μm. CNV, choroidal neovascularization; RPE, retinal pigment epithelium; WT, wild type.

Because the MAC formed as a result of complement activation is essential for the expression and release of growth factors to mediate the development of laser-induced CNV in the mouse model,[16–18] we performed experiments to compare the levels of MAC and VEGF in the retina and the choroid of the *Cd46*$^{-/-}$ and WT mice.

MAC in the Retina and Choroid of the *Cd46*$^{-/-}$ Mouse

Paraffin-embedded sections of eyes were stained with an anti-mouse C9 Ab. This Ab recognizes a neoepitope in C9 that arises when C9 is part of the MAC. We observed weak staining of the MAC in the retina (Figure 6B) and choroid (Figure 6J) of WT mice. In *Cd46*$^{-/-}$ mice, however, MAC staining was more intense in both retina and choroid (Figure 6, F and O). Increased MAC deposition on the inner surface of the retina was observed, including strong colocalization with vimentin^{+} fibrillar structures in *Cd46*$^{-/-}$ mice (Figure 6, G and H), compared with WT mice (Figure 6, C and D). We also observed increased deposition of MAC on the basal surface of CK-18^{+} RPE cells in *Cd46*$^{-/-}$ mice (Figure 6, P–R), compared with WT mice (Figure 6, K–M). No positive staining was detected in negative control section (Figure 6, A, E, I, and N). Western blot analyses confirmed the IF results, demonstrating increased C9 levels in neuronal retina, RPE, and choroid of *Cd46*$^{-/-}$ mice ($P < 0.05$) (Figure 6, S–U).

Expression of VEGF in the Retina and Choroid of the *Cd46*$^{-/-}$ Mouse

We performed IF and ELISA to assess VEGF expression in mouse retina and choroid. Using IF on paraffin-embedded sections, we observed VEGF expression in untreated WT mice in vimentin^{+} Müller cells, other retinal cells surrounding Müller cells (Figure 7, B–D), and CK-18^{+} RPE cells (Figure 7, J–M). In untreated *Cd46*$^{-/-}$ mice, expression was more intense in vimentin^{+} Müller cells (Figure 7, F–H) and in CK-18^{+} RPE cells (Figure 7, O–R). IF performed without the primary Ab demonstrated no significant staining (Figure 7, A, E, I, and N). Levels of VEGF protein, as determined by ELISA, were also significantly elevated in the neuronal retina, RPE, and choroid harvested from the eyes of untreated *Cd46*$^{-/-}$, compared with untreated WT mice ($P < 0.05$) (Figure 7S).

Discussion

Studies performed in humans and in mice, particularly over the past decade, have substantially improved our understanding of the role of the complement system in AMD.[11–24] Complement inhibitors expressed in the retina and choroid provide cellular protection during intraocular engagement of this innate immune cascade.[11–24] A decrease in this regulatory activity, for which there is strong genetic

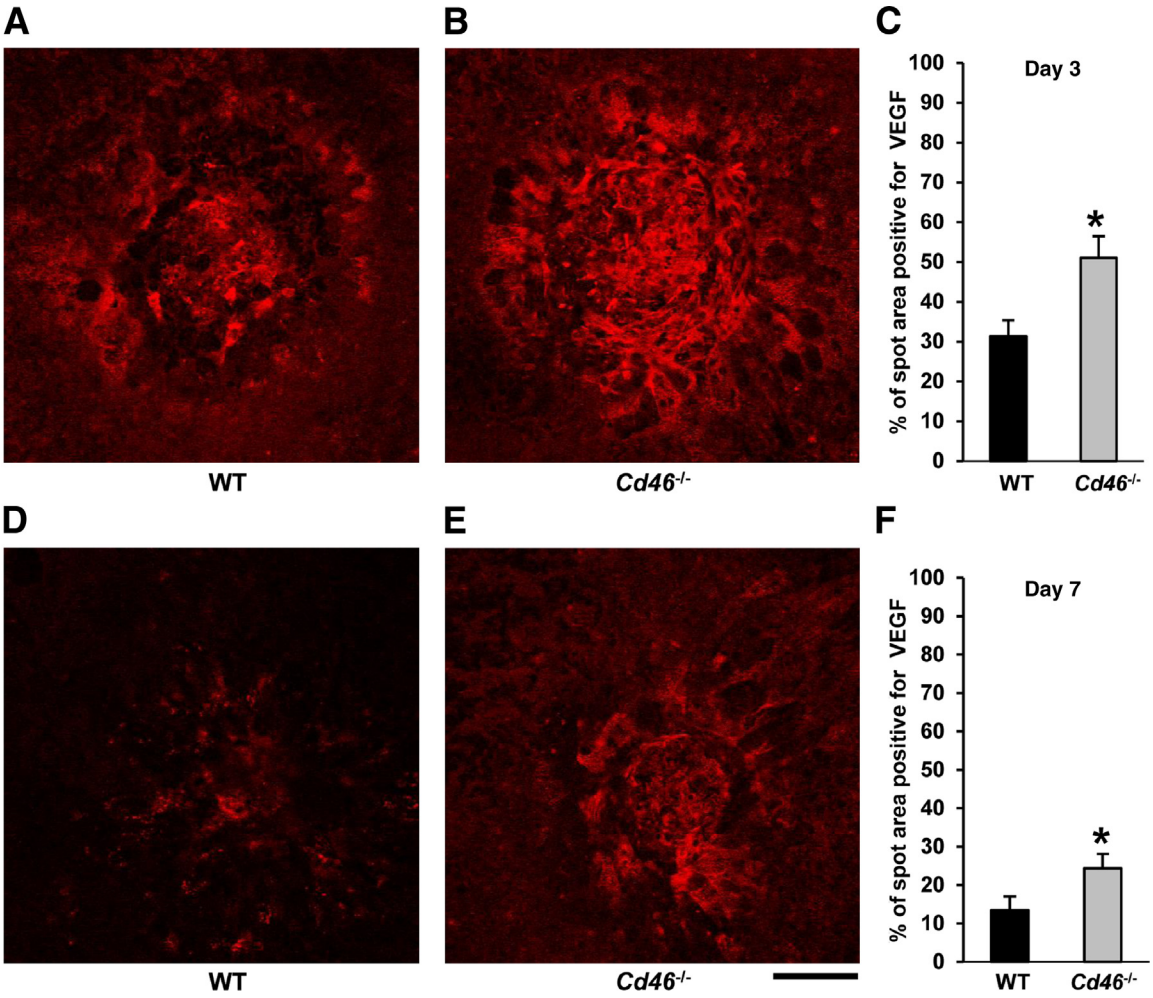

Figure 5 Effect of CD46 on VEGF expression in laser spots. **A**–**F:** CNV was induced in C57BL/6J (WT) and *Cd46*$^{-/-}$ mice by laser photocoagulation. Mice were sacrificed at days 3 and 7 after laser treatment. Representative confocal photomicrographs of RPE–choroid–scleral flat mounts with VEGF^{+} staining (red) from WT (**A** and **D**) and *Cd46*$^{-/-}$ (**B** and **E**) mice, with cumulative data of VEGF quantification (**C** and **F**). Laser-injured areas (red) in laser spots were measured using NIH ImageJ software, At both day 3 (**C**) and day 7 (**F**) after laser treatment, the VEGF^{+} area was significantly higher in *Cd46*$^{-/-}$ mice, compared with WT controls. Data are expressed as means ± SEM, representative of two independent experiments. $n = 3$ mice per group at each post-treatment time point. *$P < 0.05$. Scale bar = 100 μm. RPE, retinal pigment epithelium; WT, wild type.

evidence in humans, leads to excessive activation of the alternative complement pathway and thereby contributes to the pathology of AMD. In animal models, excessive MAC formation within the retina causes an increase in production of angiogenic growth factors that drive the development of CNV.[16–18] With the present study, we have demonstrated the expression of CD46 in multiple segments of the mouse eye and, using a *Cd46*$^{-/-}$ mouse model, we have elucidated how CD46 deficiency predisposes to more severe CNV in a laser injury model.

In humans and most other mammals, CD46 is a widely expressed membrane regulator that inhibits the alternative pathway on the same cell on which it is expressed (intrinsic protection).[26,27] CD46 accomplishes this by serving as a cofactor protein for the plasma serine protease factor I. By limited and specific proteolysis, factor I cleaves C3b bound to CD46 on a host cell. The resulting iC3b fragment cannot engage the highly efficient feedback loop of the alternative pathway,[26,27] and thus the activation process is curtailed.

The expression of CD46 in multiple locations in the human eye is well documented.[28–31] In 2003, using human donor eyes, primary cultures of human RPE, and ARPE-19 cells, we demonstrated that CD46 is preferentially localized to the basolateral surface of the RPE.[30] Other researchers have also described CD46 staining in this location in human donor eyes.[31,39,40] In mouse and rat, however, CD46 was initially reported to be expressed solely on the inner acrosomal membrane of spermatozoa, where it is also expressed in humans.[32,41] Complement receptor 1-related gene/protein-y (Crry) was hypothesized to substitute for the widely expressed CD46 in all other locations in the mouse,[42] because it is widely expressed and possesses cofactor activity for mouse C3b.

In the present study, we observed that CD46 is expressed in the retina, RPE, and choroid of the mouse eye. Two

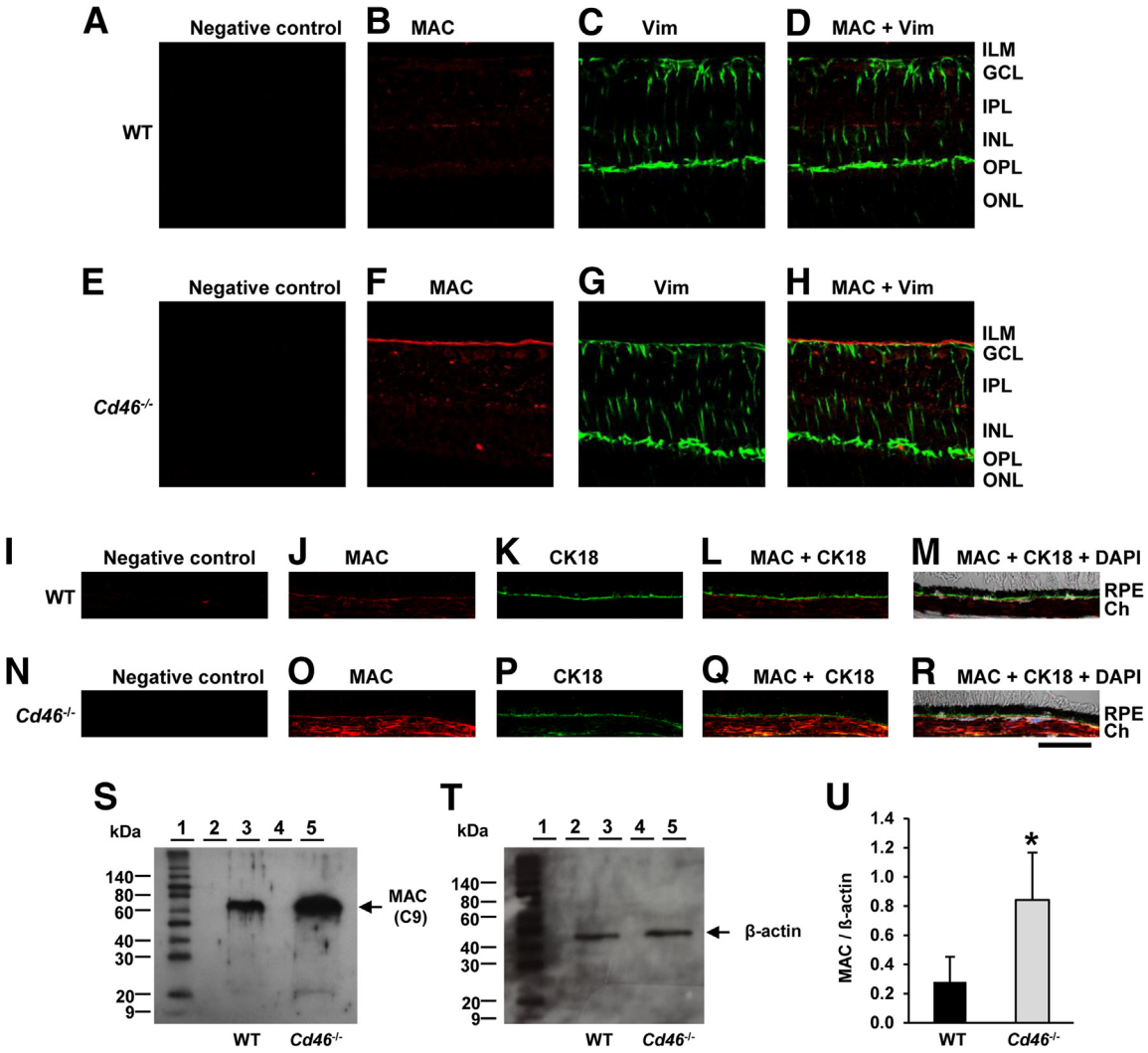

Figure 6 The MAC of complement is increased in the retina and choroid of the *Cd46*$^{-/-}$ mouse. Untreated (nonlasered) mice were used. **A**—**R:** Representative confocal photo micrographs of MAC staining (red), vimentin staining (green), and CK-18 staining (green) in paraffin-embedded sections of WT C57BL/6J neuronal retina (**A**—**D**) and RPE—choroid (**I**—**M**) and of *Cd46*$^{-/-}$ neuronal retina (**E**—**H**) and RPE—choroid (**N**—**R**). In DIC merged images (**M** and **R**), nuclei are stained with DAPI (blue). MAC staining was more intense in the retina and choroid of *Cd46*$^{-/-}$ mice (**F** and **O**), compared with WT mice (**B** and **J**). Increased MAC deposition was observed on the inner surface of the retina, including vimentin^{+} Müller cells (**H**), and on the basal surface of CK-18^{+} RPE cells (**Q** and **R**) of *Cd46*$^{-/-}$ mice, compared with WT mice (**D**, **L**, and **M**). Control sections were stained without the primary Ab (negative control) (**A**, **E**, **I**, and **N**). **S** and **T:** Representative Western blot analyses of MAC (approximately 70 kDa) and β-actin (approximately 42 kDa) in retina and choroid of WT (lane 3) and *Cd46*$^{-/-}$ (lane 5) mice. Lane 1, molecular weight marker; lanes 2 and 3, empty. Blots for MAC and β-actin were performed separately with an equivalent amount of protein loaded. **U:** Densitometric analysis of blots is expressed as the ratio of the intensity of the MAC protein to the intensity of β-actin protein band. Data are expressed as means ± SEM. Results are representative of four (**A**—**R**) or 7 (**S**—**U**) independent experiments. *$P < 0.05$. Scale bar = 40 μm. Ch, choroid. Ab, antibody; MAC, membrane attack complex; RPE, retinal pigment epithelium; WT, wild type.

recent prior reports of CD46 expression in the mouse eye do not agree on which cell types express CD46,[43,44] and in one of those studies CD46 expression was not observed in WT mice.[44] Mallam et al,[43] using immunohistochemistry and a commercially available monoclonal Ab raised to human CD46, found that CD46 is expressed in the inner and the outer segments of photoreceptors of C57BL/6J mice; however, expression at the OLM of the neurosensory retina or basolaterally on the RPE or in the choroid was not found. Ambati et al,[44] using immunohistochemistry and a commercially available rabbit polyclonal Ab raised to human CD46, observed reactivity in the eyes of aged *Ccl2*$^{-/-}$ and *Ccr2*$^{-/-}$ mice, but not in age-matched WT C57BL/6J mice. We, however, have been unable to detect specific staining in the mouse eye or spermatozoa, using these two Abs (unpublished data). In the present study, using a polyclonal Ab raised to mouse CD46, we observed specific basolateral membrane staining of the RPE, as well as CD46 expression in the retina and the choroid of WT mice. To summarize, the differences between the present study and the two other studies are likely attributable to the fact that we used an Ab directed against mouse CD46, rather than commercially available anti-CD46 Abs raised to human CD46. Furthermore, to validate our results, we had the considerable advantage of the availability of

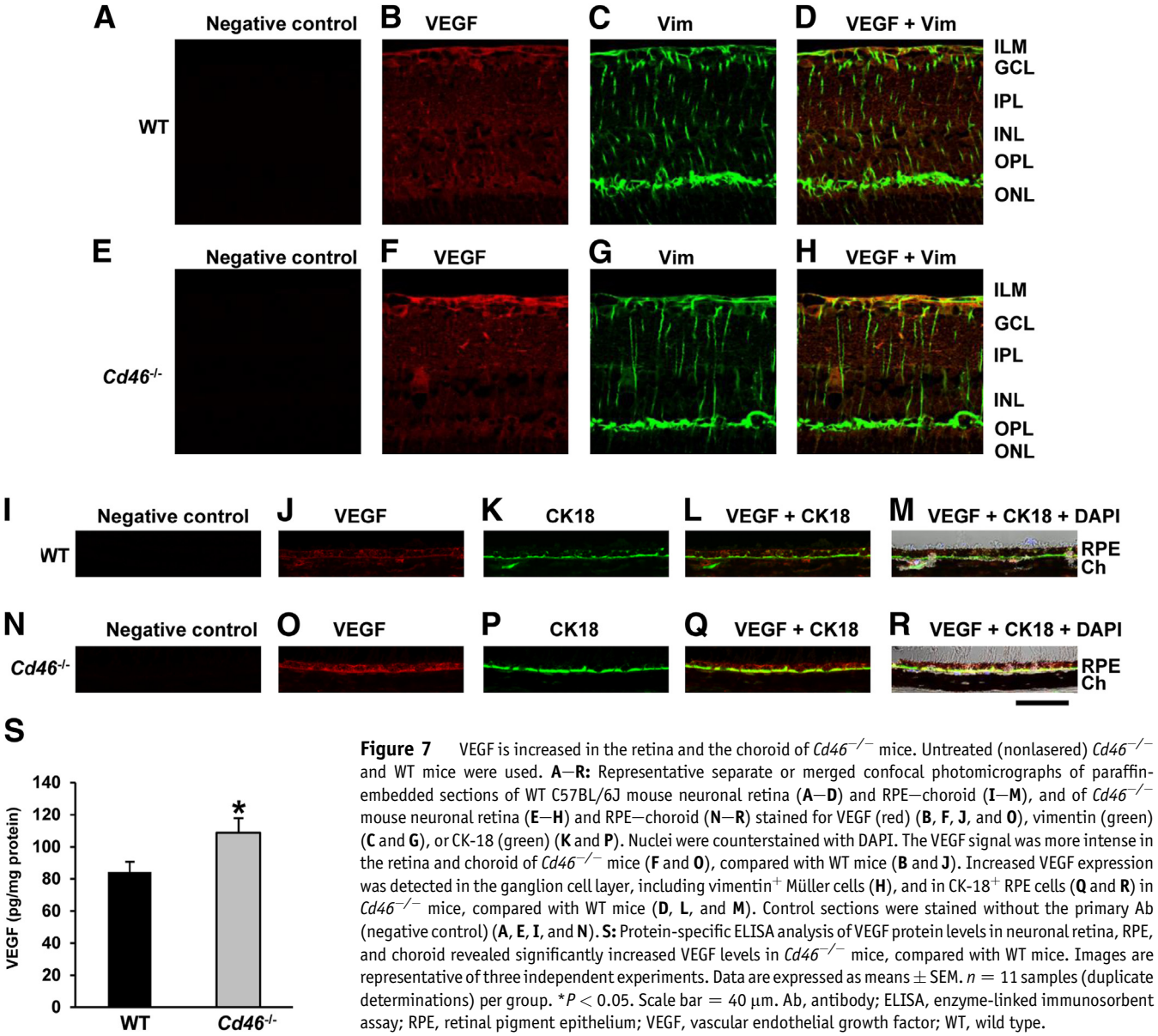

Figure 7 VEGF is increased in the retina and the choroid of *Cd46*$^{-/-}$ mice. Untreated (nonlasered) *Cd46*$^{-/-}$ and WT mice were used. **A**–**R:** Representative separate or merged confocal photomicrographs of paraffin-embedded sections of WT C57BL/6J mouse neuronal retina (**A**–**D**) and RPE–choroid (**I**–**M**), and of *Cd46*$^{-/-}$ mouse neuronal retina (**E**–**H**) and RPE–choroid (**N**–**R**) stained for VEGF (red) (**B**, **F**, **J**, and **O**), vimentin (green) (**C** and **G**), or CK-18 (green) (**K** and **P**). Nuclei were counterstained with DAPI. The VEGF signal was more intense in the retina and choroid of *Cd46*$^{-/-}$ mice (**F** and **O**), compared with WT mice (**B** and **J**). Increased VEGF expression was detected in the ganglion cell layer, including vimentin^{+} Müller cells (**H**), and in CK-18^{+} RPE cells (**Q** and **R**) in *Cd46*$^{-/-}$ mice, compared with WT mice (**D**, **L**, and **M**). Control sections were stained without the primary Ab (negative control) (**A**, **E**, **I**, and **N**). **S:** Protein-specific ELISA analysis of VEGF protein levels in neuronal retina, RPE, and choroid revealed significantly increased VEGF levels in *Cd46*$^{-/-}$ mice, compared with WT mice. Images are representative of three independent experiments. Data are expressed as means ± SEM. $n = 11$ samples (duplicate determinations) per group. $^{*}P < 0.05$. Scale bar = 40 μm. Ab, antibody; ELISA, enzyme-linked immunosorbent assay; RPE, retinal pigment epithelium; VEGF, vascular endothelial growth factor; WT, wild type.

the *Cd46*$^{-/-}$ mouse as a negative control, and we routinely used mouse testis as a positive control.

The expression pattern for CD46 in the mouse eye is of interest. The most intense staining was on the basolateral surface of RPE cells (as it is in humans[14,30,31,39,40]) and on the OLM. Also, moderate CD46 staining was present in both the inner plexiform layer and outer plexiform layer. Although it is possible that CD46 immunoreactivity at the OLM may represent accumulation of soluble CD46,[11,12,29] similar to that seen with albumin,[45] this staining pattern in the retina is, in our opinion, most consistent with CD46 localization on Müller cells, especially at terminal OLM processes. We have previously reported that the soluble form of CD46 is present in normal human vitreous.[29] Thus, the expression (or accumulation) of CD46 is polarized toward the OLM end of the Müller cells, because no staining is present at the ILM. Staining for CD46 in human neuronal retina is reported in the outer segment and inner segment of photoreceptors[28] and retinal vessels.[46] Elucidation of the nature of the variable and lighter staining pattern in choroid requires further study.

A role for CD46 in CNV was explored using *Cd46*$^{-/-}$ mice in a model of laser-induced CNV. The *Cd46*$^{-/-}$ mice had increased expression of VEGF in laser spots, compared with WT mice, and developed a more severe clinical phenotype of CNV. Recent studies analyzing CD46 expression in human eyes with the dry form of AMD indicate that CD46 is present in RPE cells overlying drusen.[14] Furthermore, in the eyes of patients with early AMD, CD46 staining was markedly reduced in RPE cells.[21,42] Those reports suggest that decreased expression of CD46 in dry AMD contributes to disease pathogenesis. Our present findings indicate that a deficiency of CD46 exacerbates CNV in mouse.

To determine why the *Cd46*$^{-/-}$ mouse is more prone to CNV, we analyzed MAC and VEGF levels. We have

previously reported that, in laser-induced CNV, MAC deposition is a major mediator of the disease process, having a direct effect on VEGF production.[16–18] Additionally, there is ample evidence in the literature that VEGF is a key angiogenic growth factor in the development of CNV, both in humans with wet AMD[47–49] and in animal models of CNV.[16–23] Our present results indicate that the MAC and VEGF are present in significantly higher amounts in the neuronal retina, RPE, and choroid of the *Cd46*$^{-/-}$ mouse. Furthermore, increased VEGF expression in Müller cells and in RPE overlapped the sites featuring elevated MAC deposition. This was prominent at the ILM as well, although our present results did not demonstrate CD46 expression in this region. We have several hypotheses about this finding, all of which would require further investigation. Either soluble CD46 present in the vitreous humor or soluble CD46 migrating through the retina from the RPE may be protective at the ILM. We even consider it possible that CD46 present at the OLM region of the Müller cells is normally protective at the ILM and in the vitreous, because it is possible that OLM membrane-bound CD46 helps to maintain tight junctions at this critical barrier through local mitigation of inflammatory factors. Absence of CD46 allows the MAC to migrate to the ILM and vitreous through a leaky barrier. This process could in turn likely up-regulate VEGF in a manner not seen in WT mice. Thus, there is an intriguing relationship among CD46 expression, MAC deposition, and elevated VEGF levels that translates into a more severe form of laser-induced CNV. We suggest that, in mice, CD46 has a role in the initiation and the progression of choroidal angiogenesis.

In conclusion, here we have reported several novel observations: i) CD46, the major membrane regulator of the human alternative pathway, is also expressed in the mouse retina, RPE, and choroid; ii) baseline levels of MAC and VEGF are increased in the retina and the choroid of mice deficient in CD46, suggesting an elevated, spontaneous basal level of complement turnover; and iii) the *Cd46*$^{-/-}$ mouse develops more severe CNV in the laser model. Taken together, these findings raise the possibility that inhibition of the alternative pathway of the complement system (eg, by recombinant CD46) could be a successful therapeutic strategy for treatment of AMD.

Acknowledgments

We thank Kathryn Liszewski for helpful suggestions and Madonna Bogacki and Lorraine Schwartz for expert secretarial assistance.

References

1. Friedman DS, O'Colmain BJ, Muñoz B, Tomany SC, McCarty C, de Jong PT, Nemesure B, Mitchell P, Kempen J; Eye Diseases Prevalence Research Group: Prevalence of age-related macular degeneration in the United States [Erratum appeared in Arch Ophthalmol 2011, 129:1188]. Arch Ophthalmol 2004, 122:564–572
2. Coleman HR, Chan CC, Ferris FL 3rd, Chew EY: Age-related macular degeneration. Lancet 2008, 372:1835–1845
3. Gehrs KM, Anderson DH, Johnson LV, Hageman GS: Age-related macular degeneration–emerging pathogenetic and therapeutic concepts. Ann Med 2006, 38:450–471
4. Christoforidis JB, Tecce N, Dell'Omo R, Mastropasqua R, Verolino M, Costagliola C: Age related macular degeneration and visual disability. Curr Drug Targets 2011, 12:221–233
5. Rein DB, Wittenborn JS, Zhang X, Honeycutt AA, Lesesne SB, Saaddine J; Vision Health Cost-Effectiveness Study Group: Forecasting age-related macular degeneration through the year 2050: the potential impact of new treatments. Arch Ophthalmol 2009, 127:533–540
6. Husain D, Ambati B, Adamis AP, Miller JW: Mechanisms of age-related macular degeneration. Ophthalmol Clin North Am 2002, 15:87–91
7. Smith W, Assink J, Klein R, Mitchell P, Klaver CC, Klein BEK, Hofman A, Jensen S, Wang JJ, de Jong PT: Risk factors for age-related macular degeneration: pooled findings from three continents. Ophthalmology 2001, 108:697–704
8. Evans JR: Risk factors for age-related macular degeneration. Prog Retin Eye Res 2001, 20:227–253
9. Khandhadia S, Cherry J, Lotery AJ: Age-related macular degeneration. Adv Exp Med Biol 2012, 724:15–36
10. Yates JR, Moore AT: Genetic susceptibility to age related macular degeneration. J Med Genet 2000, 37:83–87
11. Bora NS, Jha P, Lyzogubov VV, Bora PS: Emerging role of complement in ocular diseases. Curr Immunol Rev 2011, 7:360–367
12. Bora NS, Jha P, Bora PS: The role of complement in ocular pathology. Semin Immunopathol 2008, 30:85–95
13. Anderson DH, Radeke MJ, Gallo NB, Chapin EA, Johnson PT, Curletti CR, Hancox LS, Hu J, Ebright JN, Malek G, Hauser MA, Rickman CB, Bok D, Hageman GS, Johnson LV: The pivotal role of the complement system in aging and age-related macular degeneration: hypothesis re-visited. Prog Retin Eye Res 2010, 29:95–112
14. Johnson LV, Leitner WP, Staples MK, Anderson DH: Complement activation and inflammatory processes in drusen formation and age related macular degeneration. Exp Eye Res 2001, 73:887–896
15. Seddon JM, Yu Y, Miller EC, Reynolds R, Tan PL, Gowrisankar S, Goldstein JI, Triebwasser M, Anderson HE, Zerbib J, Kavanagh D, Souied E, Katsanis N, Daly MJ, Atkinson JP, Raychaudhuri S: Rare variants in CFI, C3 and C9 are associated with high risk of advanced age-related macular degeneration. Nat Genet 2013, 45:1366–1370
16. Bora PS, Sohn JH, Cruz JM, Jha P, Nishihori H, Wang Y, Kaliappan S, Kaplan HJ, Bora NS: Role of complement and complement membrane attack complex in laser-induced choroidal neovascularization. J Immunol 2005, 174:491–497
17. Bora NS, Kaliappan S, Jha P, Cu Q, Sohn JH, Dhaulakhandi DB, Kaplan HJ, Bora PS: Complement activation via alternative pathway is critical in the development of laser-induced choroidal neovascularization: role of factor B and factor H. J Immunol 2006, 177:1872–1878
18. Bora NS, Kaliappan S, Jha P, Xu Q, Sivasankar B, Harris CL, Morgan BP, Bora PS: CD59, a complement regulatory protein, controls choroidal neovascularization in a mouse model of wet-type age-related macular degeneration. J Immunol 2007, 178:1783–1790
19. Kaliappan S, Jha P, Lyzogubov VV, Tytarenko RG, Bora NS, Bora PS: Alcohol and nicotine consumption exacerbates choroidal neovascularization by modulating the regulation of complement system. FEBS Lett 2008, 582:3451–3458
20. Bora NS, Jha P, Lyzogubov VV, Kaliappan S, Liu J, Tytarenko RG, Fraser DA, Morgan BP, Bora PS: Recombinant membrane-targeted form of CD59 inhibits the growth of choroidal neovascular complex in mice. J Biol Chem 2010, 285:33826–33833
21. Lyzogubov VV, Tytarenko RG, Jha P, Liu J, Bora NS, Bora PS: Role of ocular complement factor H in a murine model of choroidal neovascularization. Am J Pathol 2010, 177:1870–1880

22. Lyzogubov VV, Tytarenko RG, Liu J, Bora NS, Bora PS: Polyethylene glycol (PEG)-induced mouse model of choroidal neovascularization. J Biol Chem 2011, 286:16229–16237
23. Liu J, Jha P, Lyzogubov VV, Tytarenko RG, Bora NS, Bora PS: Relationship between complement membrane attack complex, chemokine (C-C motif) ligand 2 (CCL2) and vascular endothelial growth factor in mouse model of laser-induced choroidal neovascularization. J Biol Chem 2011, 286:20991–21001
24. Liszewski MK, Atkinson JP: Regulatory proteins of complement. Edited by Volanakis J, Frank M. The Human Complement System in Health and Disease. New York, Marcel Dekker, 1998, pp 149–166
25. Morgan BP, Harris CL: Regulation in the complement system. Complement Regulatory Proteins. San Diego, Academic Press, 1999, pp 32–38
26. Liszewski MK, Leung M, Cui W, Subramanian VB, Parkinson J, Barlow PN, Manchester M, Atkinson JP: Dissecting sites important for complement regulatory activity in membrane cofactor protein (MCP; CD46). J Biol Chem 2000, 275:37692–37701
27. Liszewski MK, Kemper C, Price JD, Atkinson JP: Emerging roles and new functions of CD46. Springer Semin Immunopathol 2005, 27: 345–358
28. Bora NS, Gobleman CL, Atkinson JP, Pepose JS, Kaplan HJ: Differential expression of the complement regulatory proteins in the human eye. Invest Ophthalmol Vis Sci 1993, 34:3579–3584
29. Sohn JH, Kaplan HJ, Suk HJ, Bora PS, Bora NS: Complement regulatory activity of normal human intraocular fluid is mediated by MCP, DAF, and CD59. Invest Ophthalmol Vis Sci 2000, 41:4195–4202
30. McLaughlin BJ, Fan W, Zheng JJ, Cai H, Del Priore LV, Bora NS, Kaplan HJ: Novel role for a complement regulatory protein (CD46) in retinal pigment epithelial adhesion. Invest Ophthalmol Vis Sci 2003, 44:3669–3674
31. Fett AL, Hermann MM, Muether PS, Kirchhof B, Fauser S: Immunohistochemical localization of complement regulatory proteins in the human retina. Histol Histopathol 2012, 27:357–364
32. Riley-Vargas RC, Lanzendorf S, Atkinson JP: Targeted and restricted complement activation on acrosome-reacted spermatozoa. J Clin Invest 2005, 115:1241–1249
33. Riley-Vargas RC, Atkinson JP: Expression of membrane cofactor protein (MCP; CD46) on spermatozoa: just a complement inhibitor? Mod Asp Immunobiol 2003, 3:75–78
34. Riley RC, Kemper C, Leung M, Atkinson JP: Characterization of human membrane cofactor protein (MCP; CD46) on spermatozoa. Mol Reprod Dev 2002, 62:534–546
35. Ryan SJ: Subretinal neovascularization. Natural history of an experimental model. Arch Ophthalmol 1982, 100:1804–1809
36. Campochiaro PA: Retinal and choroidal neovascularization. J Cell Physiol 2000, 184:301–310
37. Hogan B, Beddington R, Costantini F, Lacy E: Manipulating the Mouse Embryo: A Laboratory Manual. ed 2. Cold Spring Harbor, NY, Cold Spring Harbor Laboratory Press, 1994
38. Liszewski MK, Bertram P, Leung MK, Hauhart R, Zhang L, Atkinson JP: Smallpox inhibitor of complement enzymes (SPICE): regulation of complement activation on cells and mechanism of its cellular attachment. J Immunol 2008, 181:4199–4207
39. Vogt SD, Barnum SR, Curcio CA, Read RW: Distribution of complement anaphylatoxin receptors and membrane-bound regulators in normal human retina. Exp Eye Res 2006, 83:834–840
40. Ebrahimi KB, Fijalkowski N, Cano M, Handa JT: Decreased membrane complement regulators in the retinal pigmented epithelium contributes to age-related macular degeneration. J Pathol 2013, 229:729–742
41. Tsujimura A, Shida K, Kitamura M, Nomura M, Takeda J, Tanaka H, Matsumoto M, Matsumiya K, Okuyama A, Nishimune Y, Okabe M, Seya T: Molecular cloning of a murine homologue of membrane cofactor protein (CD46): preferential expression in testicular germ cells. Biochem J 1998, 330:163–168
42. Kim YU, Kinoshita T, Molina H, Hourcade D, Seya T, Wagner LM, Holers VM: Mouse complement regulatory protein Crry/p65 uses the specific mechanisms of both human decay-accelerating factor and membrane cofactor protein. J Exp Med 1995, 181:151–159
43. Mallam JN, Hurwitz MY, Mahoney T, Chévez-Barrios P, Hurwitz RL: Efficient gene transfer into retinal cells using adenoviral vectors: dependence on receptor expression. Invest Ophthalmol Vis Sci 2004, 45:1680–1687
44. Ambati J, Anand A, Fernandez S, Sakurai E, Lynn BC, Kuziel WA, Rollins BJ, Ambati BK: An animal model of age-related macular degeneration in senescent Ccl-2- or Ccr-2-deficient mice. Nat Med 2003, 9:1390–1397
45. Vinores SA, Campochiaro PA, Lee A, McGehee R, Gadegbeku C, Green WR: Localization of blood-retinal barrier breakdown in human pathologic specimens by immunohistochemical staining for albumin. Lab Invest 1990, 62:742–750
46. Zhang J, Gerhardinger C, Lorenzi M: Early complement activation and decreased levels of glycosylphosphatidylinositol-anchored complement inhibitors in human and experimental diabetic retinopathy. Diabetes 2002, 51:3499–3504
47. Campa C, Harding SP: Anti-VEGF compounds in the treatment of neovascular age related macular degeneration. Curr Drug Targets 2011, 12:173–181
48. Kim SJ, Toma HS, Barnett JM, Penn JS: Ketorolac inhibits choroidal neovascularization by suppression of retinal VEGF. Exp Eye Res 2010, 91:537–543
49. Couch SM, Bakri SJ: Review of combination therapies for neovascular age-related macular degeneration. Semin Ophthalmol 2011, 26: 114–120